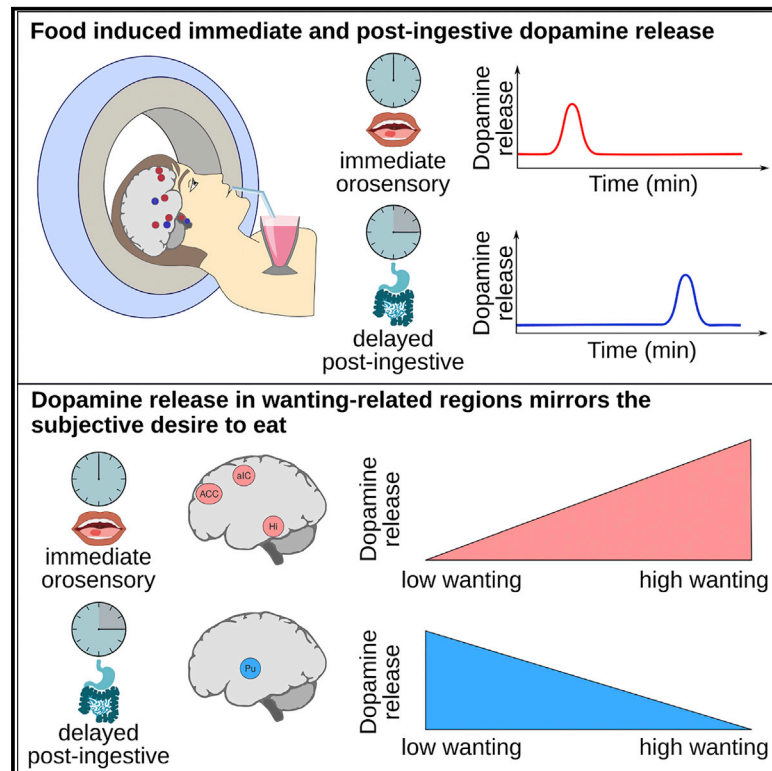


Cell Metabolism

Food Intake Recruits Orosensory and Post-ingestive Dopaminergic Circuits to Affect Eating Desire in Humans

Graphical Abstract



Authors

Sharmili Edwin Thanarajah,
Heiko Backes,
Alexandra G. DiFeliceantonio, ...,
Dana M. Small, Jens C. Brüning,
Marc Tittgemeyer

Correspondence

backes@sf.mpg.de

In Brief

Thanarajah et al. combined fMRI and PET to assess the brain's response to food intake and discovered immediate and delayed dopamine release in distinct areas of the human brain. In addition, they identified areas where dopamine release reflected subjective wanting to eat, shedding light on how the brain transforms energetic signals into the desire to eat.

Highlights

- Food intake induces orosensory and post-ingestive dopamine release in humans
- Both recruit distinct pathways: orosensory integrative and higher cognitive centers
- Dopamine release in “wanting”-associated regions mirrors subjective desire to eat
- Post-ingestive dopamine release in the putamen is inversely correlated to “wanting”

Food Intake Recruits Orosensory and Post-ingestive Dopaminergic Circuits to Affect Eating Desire in Humans

Sharmili Edwin Thanarajah,^{1,2,11} Heiko Backes,^{1,11,12,*} Alexandra G. DiFeliceantonio,^{1,3,8,10} Kerstin Albus,⁴ Anna Lena Cremer,¹ Ruth Hanssen,^{1,6} Rachel N. Lippert,¹ Oliver A. Cornely,^{4,5,9} Dana M. Small,^{3,7,8} Jens C. Brüning,^{1,4,6} and Marc Tittgemeyer^{1,4,8}

¹Max Planck Institute for Metabolism Research, Cologne, Germany

²Department of Neurology, University Hospital of Cologne, Cologne, Germany

³Department of Psychiatry, Yale University School of Medicine, New Haven, CT, USA

⁴Cologne Cluster of Excellence in Cellular Stress and Aging-Associated Disease (CECAD), Cologne, Germany

⁵Department I of Internal Medicine, University Hospital of Cologne, Cologne, Germany

⁶Center for Endocrinology, Diabetes and Preventive Medicine (CEPD), University Hospital of Cologne, Cologne, Germany

⁷Department of Psychology, Yale University, New Haven, CT, USA

⁸Modern Diet and Physiology Research Center, New Haven, CT, USA

⁹Clinical Trials Centre Cologne (ZKS Köln), University of Cologne, Cologne, Germany

¹⁰Department of Neuroscience, Icahn School of Medicine at Mount Sinai, New York, NY, USA

¹¹These authors contributed equally

¹²Lead Contact

*Correspondence: backes@sf.mpg.de

<https://doi.org/10.1016/j.cmet.2018.12.006>

SUMMARY

Pleasant taste and nutritional value guide food selection behavior. Here, orosensory features of food may be secondary to its nutritional value in underlying reinforcement, but it is unclear how the brain encodes the reward value of food. Orosensory and peripheral physiological signals may act together on dopaminergic circuits to drive food intake. We combined fMRI and a novel [¹¹C]raclopride PET method to assess systems-level activation and dopamine release in response to palatable food intake in humans. We identified immediate orosensory and delayed post-ingestive dopamine release. Both responses recruit segregated brain regions: specialized integrative pathways and higher cognitive centers. Furthermore, we identified brain areas where dopamine release reflected the subjective desire to eat. Immediate dopamine release in these wanting-related regions was inversely correlated with, and presumably inhibited, post-ingestive release in the dorsal striatum. Our results highlight the role of brain and periphery in interacting to reinforce food intake in humans.

INTRODUCTION

Recent evidence from animal models indicates that both the pleasant taste and the nutritional value of food act as reinforcers in food selection behavior (de Araujo, 2016). Highly desired food items, in turn, can enhance food intake and may lead to over-

eating and obesity (Mela, 2006). In the light of the recent obesity epidemic, a growing number of studies have investigated brain signaling mechanisms underlying food intake and their modulation by the desire to eat. However, the physiological mechanisms still remain poorly understood.

Observations in rodent models of dopamine (DA) release during active feeding (Taber and Fibiger, 1997) identified the brain's dopaminergic system as a critical mediator for the neurobiological control of food intake (Palmiter, 2007). The reinforcing properties of food seemingly arise from a complex interplay between orosensory and nutritive signals. To that end, orosensory stimulation has been demonstrated to evoke striatal DA release mediating the rewarding effect of sucrose to promote food intake in rats (Hajnal et al., 2004; Schneider, 1989; Smith, 2004). In mice, the nutritive value of food, on the other hand, is signaled post-ingestively by DA independently of taste (Tellez et al., 2013, 2016) and has the capacity to override the homeostatic control of eating (Andrews and Horvath, 2008).

For example, direct nutrient infusion into the mouse gut evokes calorie-dependent striatal DA release (Ferreira et al., 2012). Moreover, mice genetically modified to lack taste receptor signaling can develop, following repeated exposures, a similar magnitude of DA release in the ventral striatum upon sucrose ingestion as wild-type mice, reflecting nutrient association learning (de Araujo et al., 2008). Similarly, the parallel presentation of a flavor and a high-calorie gut infusion consistently induces long-lasting flavor preference (Sclafani and Ackroff, 2012) and cue-associated learning in mice (Han et al., 2016; Lucas and Sclafani, 1989). This flavor-nutrient conditioning also occurs in humans at a behavioral (Yeomans et al., 2008) and neural level (de Araujo et al., 2013). These findings suggest that orosensory features of food are secondary to its nutritional value in underlying reinforcement (de Araujo, 2016).

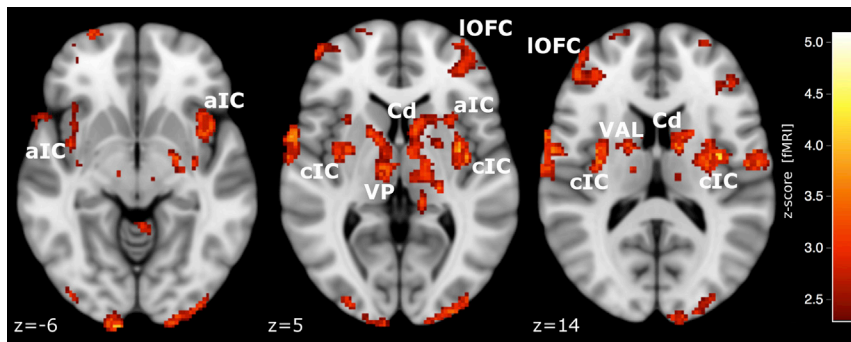


Figure 1. BOLD Activation in Response to Milkshake Intake

Compared to tasteless condition, milkshake intake elicited BOLD activation bilaterally in the anterior (aIC) as well as central insular cortex (cIC), lateral orbital frontal cortex (IOFC), ventral posterior complex of the thalamus (VP), lateral ventral anterior nucleus of the thalamus (VAL), and caudate nucleus (Cd).

To facilitate distinct orosensory and post-ingestive influences on reinforcement, segregated dopaminergic pathways are likely recruited within discrete temporal windows of action: an early window reflecting orosensation upon consumption and a second window reflecting the generation of post-ingestive signals. The latter is thought to unfold over minutes in mice (Beutler et al., 2017; Su et al., 2017) and is dependent on nutrients reaching the enteroendocrine cells in the intestine (Kaelberer et al., 2018; Tolhurst et al., 2012). Accordingly, analysis of the temporal dynamics of the blood oxygen level-dependent (BOLD) signal following glucose consumption also supports the existence of an immediate and delayed neural response (Liu et al., 2000).

Identification and discrimination of these circuits may furnish our understanding of physiological control, but also of pathophysiological dysregulation of food intake. Highly processed food with added fat and sugar is known to induce higher food wanting and overconsumption (DiFeliceantonio et al., 2018; Polk et al., 2017; Veldhuizen et al., 2017). Notably, in rodents the desire to eat (food wanting) is closely related to brain DA signaling. DA depletion in the striatum (Sotak et al., 2005) and administration of DA antagonists reduce food wanting and diminish food approach (Hsiao and Smith, 1995; Wise et al., 1978). However, as dopaminergic neuromodulation differentially impacts motor behavior and reward association (Howe and Dombek, 2016; Volkow et al., 2017), animal studies on motivational signals that determine food intake have been debated (Baldo et al., 2002; Kelley et al., 2005), especially as the behavioral readout is always conflicted by locomotion. In humans, conversely, very little is understood about the interplay between food intake, desire to eat, and brain dopamine signaling.

The majority of studies addressing food-related DA release in humans have used functional magnetic resonance imaging (fMRI; e.g., Babbs et al., 2013; O'Doherty et al., 2002; Rothenmund et al., 2007; Stice et al., 2008b; Stoeckel et al., 2008). While fMRI is advantageous in capturing brain function effectively and at a considerable spatial and temporal resolution, the respective BOLD signal is not directly related to specific neurotransmitter systems. Positron emission tomography (PET) represents a suitable technique to specifically address the dopaminergic system *in vivo*, but the application was limited by the fact that conventional analysis approaches did not allow the examination of temporal dynamics of food-induced DA release (Cosgrove et al., 2015; Small et al., 2003b; Volkow et al., 2002).

To overcome this limitation, we applied a novel method for the analysis of continuous [¹¹C]raclopride PET data that enabled us

to assess time-dependent regional DA response during and after food intake. PET as well as fMRI data were acquired

in human volunteers who received a palatable milkshake during data acquisition. With our approach, we demonstrate immediate orosensory and, for the first time, post-ingestive DA release in humans and at brain systems level. Orosensory and post-ingestive signaling recruit segregated neural circuits after food intake. We further identified brain areas where the immediate DA response was related to the desire to eat and negatively associated with post-ingestive DA release in the dorsal striatum. This suggests the existence of distinct DA mechanisms that interact over time to integrate orosensory information with post-ingestive signals regarding the nutritive value of foods. Taken together, these findings suggest a mechanism to explain how the brain transforms energetic signals into the desire to eat.

RESULTS

To investigate brain signaling during food intake we performed fMRI in 12 male, normal-weight volunteers (age, 56 ± 9.5 years; BMI, 25.57 ± 2.41 kg/m²). Ten of these participants (age, 57 ± 10.6 years; BMI, 25.73 ± 2.67 kg/m²) underwent two additional [¹¹C]raclopride PET acquisitions to characterize spatiotemporal DA release.

We acquired fMRI data during milkshake and tasteless consumption using the gustometer setup as introduced by Small et al. (2003a) and Veldhuizen et al. (2007). In line with these previous reports (cf. also de Araujo et al., 2012, for a review on orosensory-responsive brain areas), the taste of milkshake elicited activation in the anterior and central insular cortex, ventral posterior complex of the thalamus, caudate nucleus, and lateral orbitofrontal cortex, among others (Figure 1).

However, the BOLD signal is not related to a specific neurotransmitter system. Hence, we performed PET imaging with the radiolabeled D₂-receptor antagonist [¹¹C]raclopride to investigate dopamine release with the same gustometer setup providing either milkshake or tasteless solution on separate testing days. To detect any putative post-ingestive DA signaling, we continued PET acquisition for 30 min after milkshake or tasteless delivery was completed (Figure S1). Subsequently, we calculate the regional DA release rate (rDA) from [¹¹C]raclopride data. Milkshake-induced DA release was assessed by performing a voxel-wise paired t test between rDA in response to milkshake and tasteless consumption for each 5-min time interval.

We first determined time intervals with increased DA release related to milkshake consumption by plotting the number of

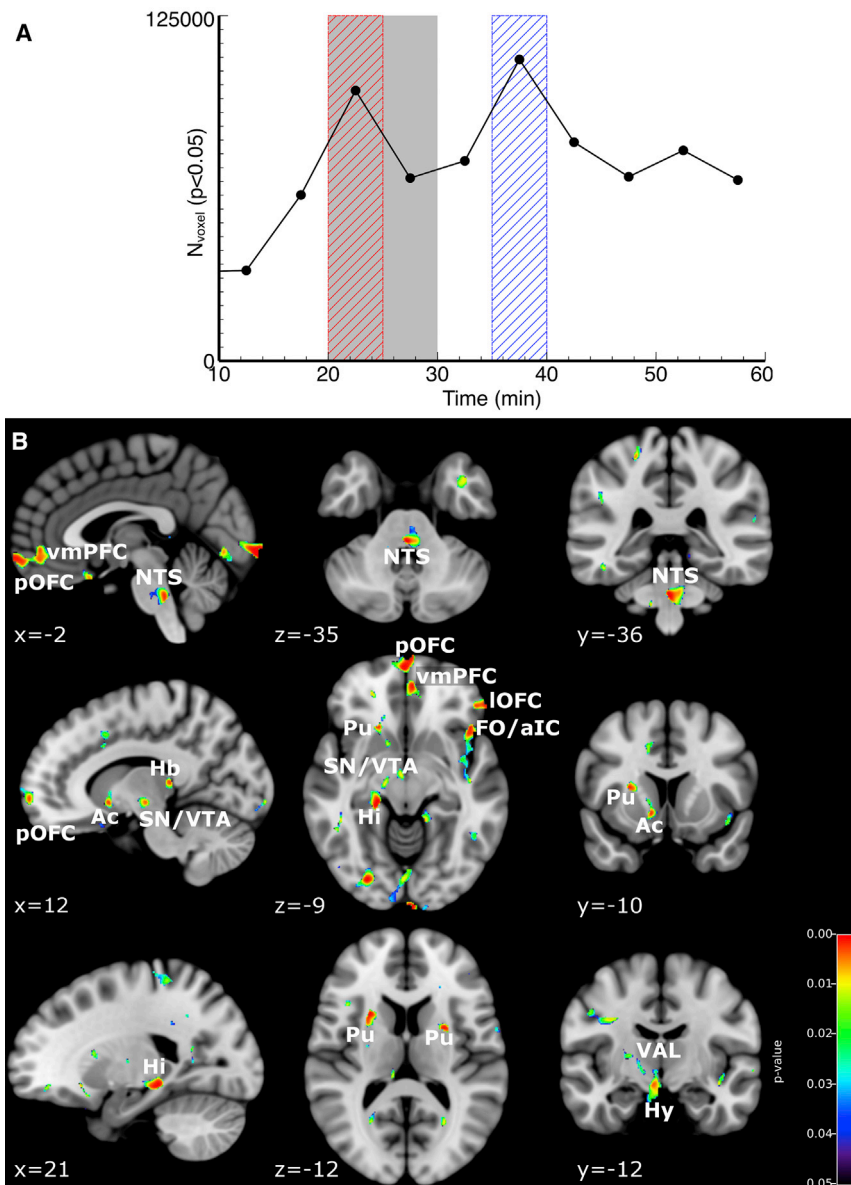


Figure 2. DA Response to Milkshake Intake

(A) Time intervals of food-induced DA response. Number of voxels with significantly increased rDA in milkshake versus tasteless condition. The data indicate an immediate (20–25 min, red box) and a delayed (35–40 min, blue box) time interval of food-induced dopaminergic activation. The gray box indicates the time of milkshake/tasteless solution supply.

(B) Immediate DA response. Immediately after milkshake delivery was initiated, rDA increased in the polar (pOFC) and lateral (lOFC) orbitofrontal cortex, nucleus of the solitary tract (NTS), nucleus accumbens (Ac), putamen (Pu), substantia nigra/ventral tegmental area (SN/VTA), lateral ventral anterior nucleus of the thalamus (VAL), habenular complex (Hb), frontal operculum/anterior insular cortex (FO/aIC), hippocampus (Hi), ventromedial prefrontal cortex (vmPFC), and hypothalamus (Hy) (Table 1). The maps are thresholded at $p < 0.05$ (whole-brain analysis; time interval, 20–25 min).

medial prefrontal cortex, lateral orbitofrontal cortex), memory (hippocampus), and inhibitory control (lateral ventral anterior nucleus of the thalamus, habenula; Figure 2B; Table 1). However, 15–20 min after milkshake consumption, DA release occurred in a distinct brain circuit including the anterior insula, ventral posterior medial nucleus of the thalamus, caudate nucleus, pallidum (external segment), amygdala (basolateral complex), parietal operculum, dorsomedial prefrontal cortex, anterior prefrontal cortex, and lateral caudal pontine nuclei (Figure 3; Table 2).

To analyze the interaction between immediate and delayed DA release, we performed a pairwise correlation analysis between immediate and delayed responding regions. Immediate DA release in the nucleus accumbens predicted later DA release in the caudate nucleus ($p = 0.037$, $r = 0.66$; Figure 3B).

significantly increased voxels over time following a temporal clustering method introduced by Liu et al. (2000). Corresponding to Liu et al. (2000), we identified two time intervals of neural response: the first immediately after application of milkshake or tasteless solution (20–25 min); the second 15–20 min after onset and accordingly 5–10 min after offset of milkshake or tasteless solution intake (35–40 min; Figure 2A).

In a whole-brain analysis, we next focused on these two time intervals to identify brain circuitries involved in the immediate and delayed DA release (15–20 min after food intake). With onset of milkshake delivery, DA release was increased in the lateral hypothalamus and dorsal striatum (bilateral putamen) as well as in orosensory pathways (including the frontal operculum/anterior insular cortex, nucleus of the solitary tract), mesolimbic DA system (nucleus accumbens, substantia nigra/ventral tegmental area [SN/VTA] complex), areas involved in reward value signaling (ventro-

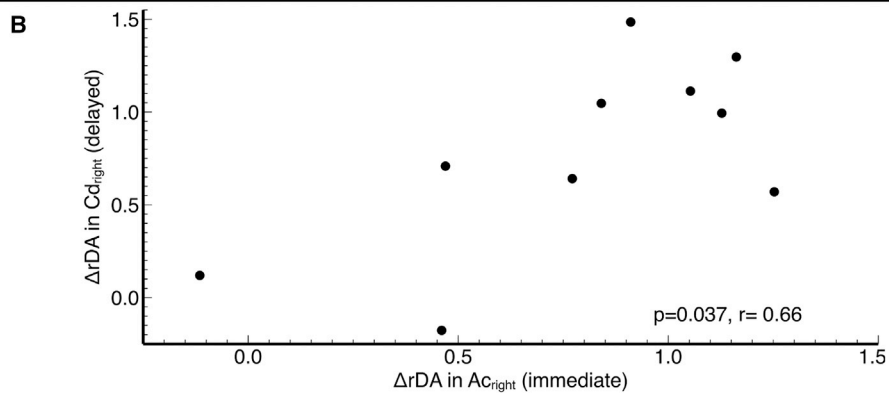
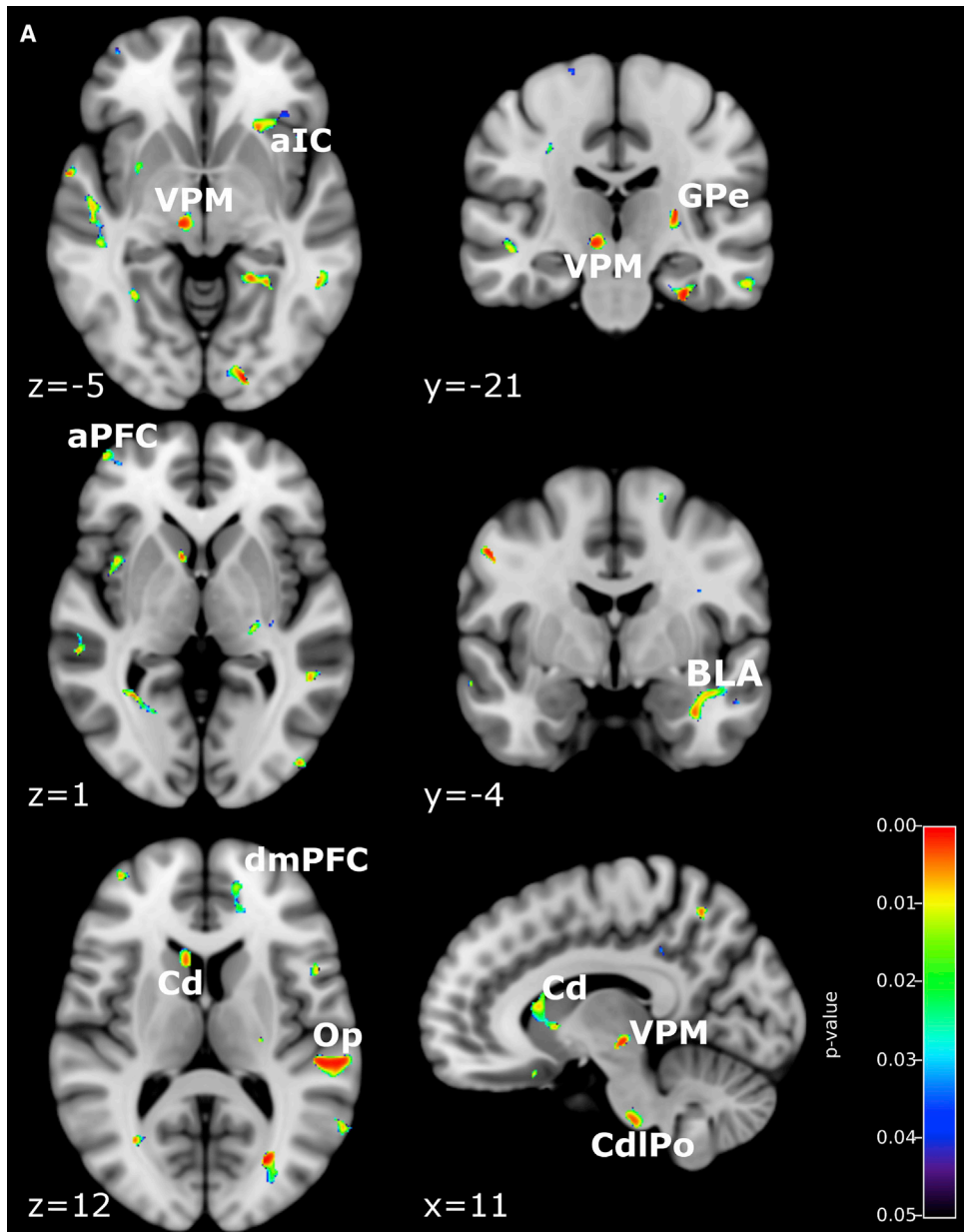
To identify BOLD activation related to DA release, we compared group statistics of immediate DA release with the corresponding fMRI response (milkshake-tasteless). We found an overlap of activations for both modalities in the anterior insular cortex, SN/VTA complex, and occipital cortex. Interestingly, a widespread network of brain areas showed activation in the fMRI data without overlapping PET response, possibly due to the engagement of other neurotransmitter systems: lateral ventral anterior and ventral posterior medial nucleus of the thalamus, claustrum, and anterior prefrontal cortex (Figure 4).

To elucidate whether measures of eating desire were related to immediate and late DA release, we performed a voxel-wise correlation analysis between the wanting score and difference between rDA after milkshake and tasteless solution intake (ΔrDA). The wanting score was highly correlated with the immediate ΔrDA in the anterior insular cortex ($p = 0.0002$, $r = 0.94$),

Table 1. Areas Showing DA Release Immediately after Milkshake Intake

| Area | Hemisphere | x | y | z | Number of Voxels | Mean rDA (Tasteless) | Mean rDA (Milkshake) | % Increase | P _{Uncorr} (min) | P _{FWE} (min) | P _{Uncorr} (Cluster) | P _{FWE} (Cluster) |
|--|------------|-----|-----|-----|------------------|----------------------|----------------------|------------|---------------------------|------------------------|-------------------------------|----------------------------|
| Ventromedial prefrontal cortex (vmPFC) | left | -1 | 48 | -10 | 555 | 0.0842 ± 0.0426 | 0.1432 ± 0.0596 | 70.0 | 0.00027 | 0.00048 ^a | 0.00001 | 0.00000 ^a |
| Orbitofrontal cortex (polar part, pOFC) | right | 4 | 58 | -14 | 612 | 0.0974 ± 0.0565 | 0.1819 ± 0.0842 | 86.8 | 0.00018 | 0.00005 ^a | 0.00030 | 0.00000 ^a |
| Cingulate gyrus (CG) | right | 11 | 18 | 39 | 280 | 0.0852 ± 0.0341 | 0.1369 ± 0.0599 | 60.7 | 0.01147 | 1.00000 | 0.00391 | 0.00933 ^a |
| Dorsomedial prefrontal cortex (dmPFC) | left | -8 | 51 | 21 | 407 | 0.0736 ± 0.0372 | 0.1220 ± 0.0588 | 65.7 | 0.00232 | 0.50764 | 0.00198 | 0.00007 ^a |
| Anterior insular cortex (aIC) | left | -44 | 18 | -9 | 490 | 0.0964 ± 0.0491 | 0.1821 ± 0.0742 | 88.8 | 0.00018 | 0.00005 ^a | 0.00018 | 0.00000 ^a |
| | right | 39 | 20 | 8 | 305 | 0.0777 ± 0.0430 | 0.1253 ± 0.0482 | 61.2 | 0.00037 | 0.00159 ^a | 0.00208 | 0.00042 ^a |
| Central insular cortex (cIC) | left | -39 | 2 | -9 | 66 | 0.0954 ± 0.0495 | 0.1466 ± 0.0530 | 53.6 | 0.01135 | 1.00000 | 0.00684 | 0.66303 |
| Hypothalamus (Hy) | right | 6 | -11 | -12 | 245 | 0.1041 ± 0.0623 | 0.2064 ± 0.1087 | 98.3 | 0.00229 | 0.49845 | 0.00318 | 0.00651 ^a |
| Substantia nigra/ventral tegmental area (SN/VTA) | right | 11 | -15 | -5 | 270 | 0.0989 ± 0.0498 | 0.1843 ± 0.0773 | 86.3 | 0.00327 | 1.00000 | 0.00120 | 0.00005 ^a |
| Lateral orbitofrontal cortex (lOFC) | left | -49 | 38 | -7 | 302 | 0.0974 ± 0.0425 | 0.1662 ± 0.0655 | 70.7 | 0.00061 | 0.00885 ^a | 0.00252 | 0.00107 ^a |
| Nucleus accumbens (Ac) | right | 11 | 8 | -7 | 215 | 0.0489 ± 0.0322 | 0.0831 ± 0.0443 | 70.1 | 0.00180 | 0.26544 | 0.00234 | 0.00292 ^a |
| Putamen (Pu) | right | 26 | 10 | 12 | 259 | 0.0714 ± 0.0382 | 0.1134 ± 0.0316 | 58.9 | 0.00027 | 0.00042 ^a | 0.00040 | 0.00000 ^a |
| | left | -24 | 4 | 13 | 275 | 0.0467 ± 0.0200 | 0.0863 ± 0.0407 | 84.8 | 0.00037 | 0.00123 ^a | 0.00050 | 0.00000 ^a |
| Hippocampus (Hi) | right | 21 | -31 | -7 | 260 | 0.0996 ± 0.0505 | 0.1877 ± 0.0709 | 88.4 | 0.00003 | 0.00000 ^a | 0.00019 | 0.00000 ^a |
| Parahippocampal gyrus (PHG) | right | 2 | -81 | -5 | 100 | 0.0846 ± 0.0512 | 0.1716 ± 0.0728 | 102.9 | 0.00024 | 0.00021 ^a | 0.00024 | 0.00000 ^a |
| Habenula (Hb) | right | 11 | -30 | 7 | 284 | 0.1021 ± 0.0453 | 0.1668 ± 0.0754 | 63.4 | 0.00186 | 0.29509 | 0.00215 | 0.00068 ^a |
| Nucleus of the solitary tract (NTS) | left | -2 | -35 | -35 | 339 | 0.1272 ± 0.0543 | 0.2807 ± 0.1347 | 120.6 | 0.00021 | 0.00014 ^a | 0.00283 | 0.00110 ^a |
| Fusiform gyrus (middle part, FuG) | right | 46 | -44 | -16 | 370 | 0.0879 ± 0.0360 | 0.1558 ± 0.0740 | 77.3 | 0.00015 | 0.00004 ^a | 0.00054 | 0.00000 ^a |
| | left | -49 | -44 | -15 | 51 | 0.0792 ± 0.0282 | 0.1193 ± 0.0376 | 50.5 | 0.00229 | 0.49002 | 0.00329 | 0.18747 |
| Precentral gyrus (PrG) | right | 42 | -7 | 30 | 275 | 0.0693 ± 0.0259 | 0.1273 ± 0.0694 | 83.7 | 0.00650 | 1.00000 | 0.00924 | 0.18901 |
| Ventral anterior nucleus of the thalamus (VAL) | right | 22 | -11 | 7 | 52 | 0.0820 ± 0.0343 | 0.1256 ± 0.0499 | 53.3 | 0.01199 | 1.00000 | 0.00120 | 0.00005 ^a |

^ap < 0.05



(legend on next page)

hippocampus ($p = 0.0002$, $r = 0.94$), and anterior cingulate cortex (ACC; $p = 0.0006$, $r = 0.91$; [Figure 5A](#)). The correlation with the delayed signal showed an opposite effect. Here, the wanting score predicted diminished ΔrDA in the putamen ($p = 0.00005$, $r = -0.96$; [Figure 5B](#)). Consequently, there was also a negative correlation between combined early ΔrDA in the anterior insula cortex, hippocampus, and ACC as well as the late ΔrDA in the putamen ($p = 0.0001$, $r = -0.93$), although this analysis included additional PET data from one subject who did not perform the wanting rating.

Next, we tested the correlation between dopaminergic activity in the areas associating with food wanting (anterior insular cortex, hippocampus, ACC) at the time of food intake—milkshake or tasteless solution—and the post-ingestive dopaminergic activity in the putamen ([Figure 5D](#)). Independent of the stimulus (tasteless or milkshake) the immediate DA release in the wanting-related regions was negatively correlated with the post-ingestive DA release in the putamen (milkshake, $p = 0.008$, $r = -0.78$; tasteless solution, $p = 0.007$, $r = -0.78$).

To control for differences in the internal states between testing days and time points, we instructed the participants to rate hunger, satiety, and tiredness. The ratings in baseline condition and the repeated measures after PET or fMRI acquisition did not show a difference between testing days or time points (pre- and post-scan).

To ensure adherence to overnight fast and to control for putative metabolic influences, we acquired insulin and glucose level in the baseline conditions of both fMRI and PET scans. None of the parameters showed a significant difference between the testing days. Moreover, the glucose level acquired before and after the gustometer task did not differ on all three testing days.

DISCUSSION

It is generally assumed that both taste and nutritional value influence food-related DA signaling, but the underlying mechanisms and functional consequences remained unclear. By applying a novel method for the analysis of [^{11}C]raclopride PET data, we provide evidence for an immediate and delayed DA release in segregated brain areas after food intake in humans.

The sensation of pleasant taste immediately elicited DA release in the orosensory pathway comprising the nucleus of the solitary tract, lateral ventral anterior nucleus of the thalamus, and frontal operculum/anterior insular cortex. These findings extend previous human and animal work on orosensory perception ([Chen et al., 2011](#); [de Araujo and Simon, 2009](#)), and provide evidence that the BOLD activation of the insular cortex reported in previous studies indeed relates to DA release ([Frank et al., 2016](#); [Small et al., 2003a](#); [Veldhuizen et al., 2011](#)). The frontal operculum/anterior insular cortex is the primary gustatory cortex, and the DA release that straddles the entire ventral agranular insula ([Evrard et al., 2014](#)) integrates multi-sensory information

and motivation-related circuitry ([de Araujo et al., 2012](#); [Maffei et al., 2012](#); [Small et al., 2004](#)). Congruent with these assumptions, our data revealed DA release in key regions of motivated behavior, reward valuation, and inhibitory control, such as the SN/VTA complex, nucleus accumbens, putamen, ventromedial prefrontal cortex, orbitofrontal cortex, hippocampus, and habenula ([Assar et al., 2016](#); [Baker et al., 2016](#); [Berridge and Robinson, 1998](#); [Kenny, 2011](#); [Palmiter, 2007](#)). Moreover, we found a strong DA release in the hypothalamus, tentatively in the lateral hypothalamus. This is interesting in the context of recent studies highlighting the role of lateral hypothalamus in integrating reward and feeding-specific circuits ([Stuber and Wise, 2016](#)) and disseminating information about reward-predictive cues ([Sharpe et al., 2017](#)). The fact that release was observed in the early “sensory” phase is also consistent with findings in mice showing that sensory detection of food activates agouti-related protein (AgRP) and proopiomelanocortin (POMC) hypothalamic neurons even before food is consumed ([Chen et al., 2015](#)). Collectively, this pattern of activation suggests that the immediate DA signals orosensory, homeostatic, and reinforcing features of food perceived in the oral cavity and highlights a role for the hypothalamus in responding to the sensory properties of foods.

Fifteen to twenty minutes after milkshake intake, we discovered a delayed DA release in a different circuit including the caudate head, pallidum, basolateral amygdala, ventral posterior medial thalamus, anterior insula, anterior and dorsomedial prefrontal cortex, and lateral caudate pontine nucleus. The temporal delay suggests that the second peak is mediated by post-ingestive signaling. Our finding thereby supports the current view based on rodent studies that the nutritional value of food primarily affects feeding by modulating dopaminergic pathways through gut-derived signals also in humans. According to previous microdialysis data in mice showing calorie-dependent DA release in the dorsal striatum after gastric infusion ([Tellez et al., 2013](#)), we identified a strong DA signal in the caudate head after milkshake consumption. In our data, DA release was also evident in areas representing interoceptive signaling from throughout the body as well as state-specific biased processing of motivationally relevant cues (insular cortex, ventral posterior medial thalamus, and basolateral amygdala; cf. [Livneh et al., 2017](#)), corticopontine pathways concerned with multiple domains of higher-order processing (dorsomedial and anterior prefrontal cortex, lateral caudate pontine nucleus; see [Schmahmann and Pandya, 1997](#)), and areas associated with goal-directed behavior and affective processing (dorsal caudate, pallidum; [Balleine et al., 2007](#); [Delgado et al., 2004](#)).

Collectively, these findings provide first evidence for post-ingestive DA release in humans and stress the relevance of higher cognitive centers in control of food intake. Furthermore, our data support the concept that brain DA circuits serve as a nutritional sensor and guide food control by reinforcing highly nutritive food stimuli ([Pignatelli and Bonci, 2015](#)). In light of the

Figure 3. Delayed DA Release

(A) Twenty minutes after milkshake consumption, rDA release raised in the caudate nucleus (Cd), pallidum (external segment; GPe), anterior insular cortex (aIC), ventral posterior medial nucleus of the thalamus (VPM), amygdala (basolateral complex; BLA), parietal operculum (Op), anterior and dorsomedial prefrontal cortex (aPFC and dmPFC), and lateral caudal pontine nucleus (CdIPo). The maps are thresholded at $p < 0.05$ (whole brain; time interval, 40–45 min) ([Table 2](#)). (B) Correlation between the immediate difference between rDA in the milkshake and the tasteless condition (ΔrDA) in nucleus accumbens (Ac) correlates with delayed ΔrDA in the caudate nucleus (Cd).

Table 2. Areas Showing DA Release 20 min after Milkshake Intake

| Area | Hemisphere | x | y | z | Number of Voxels | Mean rDA (Tasteless) | Mean rDA (Milkshake) | % Increase | P _{Uncorr} (min) | P _{FWE} (min) | P _{Uncorr} (Cluster) | P _{FWE} (Cluster) |
|--|------------|-----|-----|-----|------------------|----------------------|----------------------|------------|---------------------------|------------------------|-------------------------------|----------------------------|
| Anterior insular cortex (aIC) | left | -25 | 23 | -5 | 140 | 0.0633 ± 0.0307 | 0.1159 ± 0.0544 | 83.1 | 0.00214 | 0.41236 | 0.00233 | 0.01048 ^a |
| | right | 31 | 18 | -11 | 256 | 0.0865 ± 0.0418 | 0.1659 ± 0.0756 | 91.8 | 0.00052 | 0.00488 ^a | 0.00038 | 0.00000 ^a |
| Caudate nucleus (Cd) | right | 11 | 18 | 9 | 361 | 0.0697 ± 0.0298 | 0.1232 ± 0.0540 | 76.7 | 0.00122 | 0.08886 | 0.00231 | 0.00031 ^a |
| Operculum (Op) | left | -52 | -29 | 10 | 759 | 0.0836 ± 0.0354 | 0.1607 ± 0.0729 | 92.1 | 0.00012 | 0.00002 ^a | 0.00008 | 0.00000 ^a |
| Subthalamic nucleus (STh) | right | 10 | -20 | -4 | 252 | 0.0983 ± 0.0543 | 0.1719 ± 0.0785 | 74.8 | 0.00113 | 0.06832 | 0.00433 | 0.01952 ^a |
| Nucleus accumbens (Ac) | right | 10 | 11 | 0 | 23 | 0.0674 ± 0.0294 | 0.1093 ± 0.0430 | 62.2 | 0.00122 | 0.08886 | 0.00175 | 0.06889 |
| Amygdala (basolateral portion; Amg) | left | -34 | -5 | -24 | 379 | 0.0866 ± 0.0328 | 0.1566 ± 0.0642 | 80.9 | 0.00204 | 0.36735 | 0.00029 | 0.00000 ^a |
| Anterior prefrontal cortex/frontal pole (aPFC) | right | 41 | 58 | -1 | 303 | 0.0639 ± 0.0247 | 0.1118 ± 0.0467 | 74.9 | 0.00040 | 0.00205 ^a | 0.00076 | 0.00000 ^a |
| Dorsomedial prefrontal cortex (dmPFC) | left | -9 | 50 | 23 | 232 | 0.0676 ± 0.0333 | 0.1202 ± 0.0542 | 77.8 | 0.00217 | 0.42912 | 0.00296 | 0.00588 ^a |
| Precentral gyrus (PrG) | left | -46 | 24 | 28 | 247 | 0.0857 ± 0.0427 | 0.1501 ± 0.0729 | 75.1 | 0.00137 | 0.12594 | 0.00171 | 0.00042 ^a |
| Central insular cortex (cIC) | right | 37 | 5 | 1 | 174 | 0.0831 ± 0.0376 | 0.1482 ± 0.0717 | 78.4 | 0.00610 | 1.00000 | 0.00623 | 0.16587 |
| Substantia nigra/ventral tegmental area (SN/VTA) | right | 10 | -16 | -9 | 134 | 0.0950 ± 0.0543 | 0.1763 ± 0.0787 | 85.5 | 0.00113 | 0.06832 | 0.00270 | 0.02017 ^a |
| Pallidum (external segment, GPe) | left | -25 | -17 | 8 | 203 | 0.0734 ± 0.0352 | 0.1190 ± 0.0553 | 62.0 | 0.00003 | 0.00000 ^a | 0.00147 | 0.00046 ^a |
| Hippocampus (Hi) | right | 39 | -26 | -17 | 308 | 0.0945 ± 0.0381 | 0.1647 ± 0.0619 | 74.3 | 0.00018 | 0.00005 ^a | 0.00011 | 0.00000 ^a |
| | left | -39 | -26 | -10 | 302 | 0.0960 ± 0.0350 | 0.1591 ± 0.0674 | 65.6 | 0.00174 | 0.24616 | 0.00224 | 0.00062 ^a |
| Thalamus (ventral posteromedial nucleus, VPM) | right | 9 | -23 | -3 | 221 | 0.0978 ± 0.0541 | 0.1731 ± 0.0786 | 77.0 | 0.00113 | 0.06832 | 0.00381 | 0.01825 ^a |
| Lateral caudate pontine nucleus (CdIPo) | right | 13 | -27 | -38 | 307 | 0.1405 ± 0.0652 | 0.2314 ± 0.0953 | 64.7 | 0.00107 | 0.06109 | 0.00102 | 0.00001 ^a |

^ap < 0.05

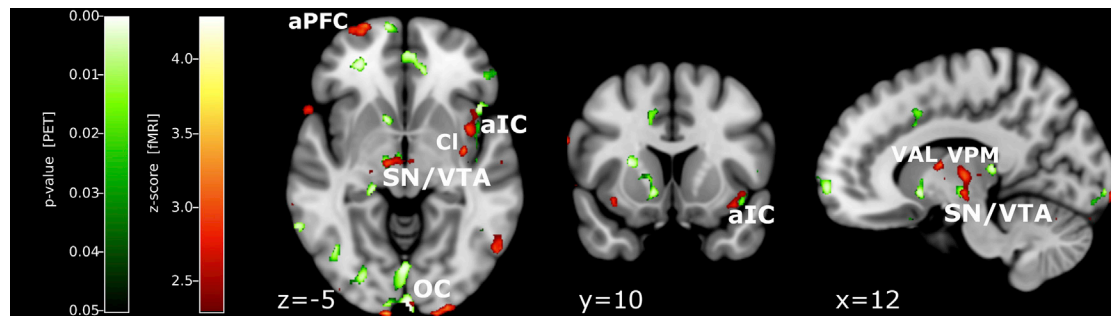


Figure 4. Combined fMRI and PET Analysis

The fMRI-BOLD activation (red scale) overlapped with DA release (green scale) in the anterior insular cortex (aIC), substantia nigra/ventral tegmental area (SN/VTA), and occipital cortex (OC). BOLD activation in the fMRI data occurs without overlapping primarily in the claustrum (Cl) and in the ventroanterior (VAL) and ventral posterior medial nucleus (VPM) of the thalamus as well as in the anterior prefrontal cortex. Both maps were derived from group statistics for the contrast milkshake-tasteless. The DA release was assessed in the early time interval (20–25 min), thresholded at $p < 0.05$. The fMRI map was derived from z-statistics at group level and thresholded for $z > 2.3$.

literature we review in the introduction, it is interesting that immediate and post-ingestive response recruit anatomically segregated structures in the striatum, highlighting different roles in action-reward associations in decision-making and reward dependence to continue previously rewarded behavior (Balleine et al., 2007; Cohen et al., 2009). This mechanism is further substantiated through a correlation between delayed activation in the caudate head and immediate activation in the nucleus accumbens, suggesting a stronger brain response to the taste of milkshake depending on its learned nutritional value.

The desire to eat has a strong impact on food selection and the amount of food that we eat even beyond metabolic demands. We identified a set of brain regions in which DA release was strongly correlated with the subjective desire to eat. Higher wanting scores predicted enhanced orosensory DA release in motivation-associated areas comprising the ACC, hippocampus, and insular cortices (Murdaugh et al., 2012; Robinson et al., 2016) and diminished post-ingestive DA release in the putamen. Surprisingly, even irrespective of milkshake or tasteless solution intake, DA release in the regions related to wanting score at food intake was inversely correlated with post-ingestive DA release in the putamen (Figure 5D). Therefore, high desire to eat and thus high DA release in wanting-related areas presumably inhibits post-ingestive DA release in the putamen—a scenario illustrated in Figure 5E. A potential interpretation for this mechanism is that wanting suppresses satiety-related signaling, which would then lead to overconsumption of highly desired food. This hypothesis, however, requires further investigation.

The current findings also have high relevance for understanding the obesity epidemic. Prolonged high-fat diet and compulsive eating as well as weakened impulse control are associated with D2-receptor downregulation in rodents (Adams et al., 2015; Johnson and Kenny, 2010; van de Giessen et al., 2013) and reduced striatal activation in response to food consumption in humans (Babbs et al., 2013; Stice et al., 2008a; Volkow et al., 2017). Nutrient sensing in DA circuits is critical for learned food preferences and directly involved in the initiation of feeding motor programs (Tellez et al., 2016). Hence, post-ingestive DA deficiency in obesity has behavioral consequences. In rodents,

it was associated with reduced motivated food-seeking behavior and increased preference for high caloric food (Tellez et al., 2013). The behavioral consequences of wanting-dependent DA release reported in our study have to be investigated in future studies.

In conclusion, we demonstrate evidence for immediate orosensory and delayed post-ingestive DA release in separate neural circuits after food intake in humans at a brain systems level. While the immediate DA response recruits specialized orosensory integrative pathways, post-ingestive DA signaling acts on higher cognitive centers and mediates their modulation by the internal state of the body, stressing therefore their central role in food intake regulation. Furthermore, we showed that DA release in wanting-related areas at food intake mirrored subjective desire to eat and presumably inhibited post-ingestive DA release in the putamen.

Limitations of Study

Given that the density of D2 receptors in extrastriatal regions is only $<10\%$ of the density in the striatum, it may be questionable if low-affinity tracers such as [11C]raclopride are able to detect DA release outside of the striatum. However, there are two factors that promote detection of extrastriatal DA release with the novel method. First, the method relates relative variations of the [11C]raclopride signal and not the absolute signal to DA release events. By comparison of intra- and extrastriatal [11C]raclopride kinetics and its responsiveness to minute-by-minute temporal variations of extracellular DA concentrations, we could show, with the help of model calculations, that although the D2 density is more than a factor of 10 lower outside of the striatum, the amplitude of temporal variations of [11C]raclopride is only a factor of 5 lower in these regions (Lippert et al., 2018). Second, [11C]raclopride solely responds to slow variations of extracellular DA concentrations. *In situ* voltammetric recordings in the striatum of rodents indeed show that part of the DA that diffuses into extracellular space after phasic release is removed at a minute timescale. We hypothesized that this slow removal rate originates from subcellular compartments in the extracellular space with low density of DA transporters. Extrastriatal regions have a lower density not only of DA synapses and DA receptors but also of DA transporters.

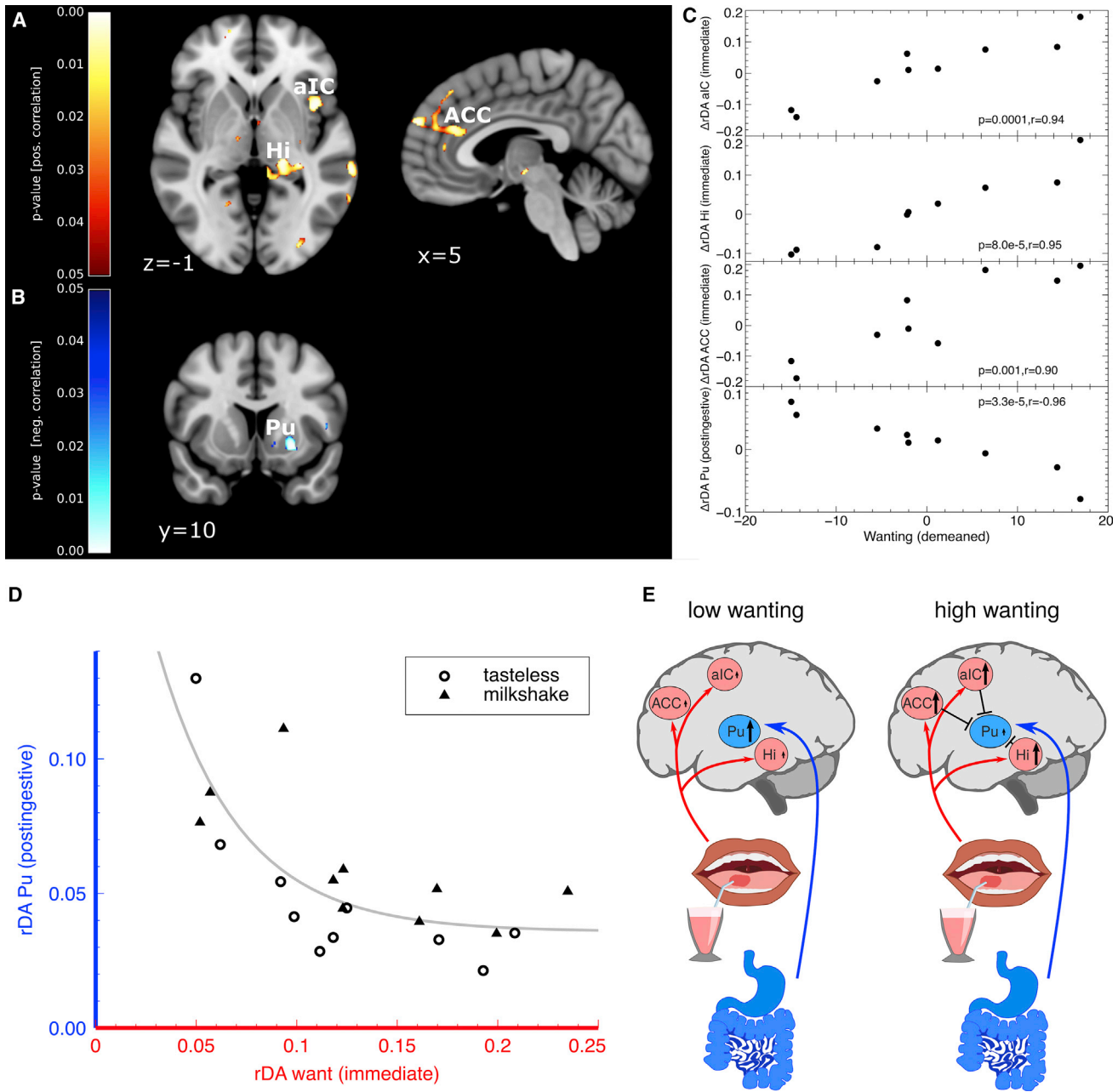


Figure 5. Measures of Wanting and DA Response

(A) Correlation between wanting ratings and the difference between immediate DA release after milkshake and tasteless solution intake (ΔrDA ; 20–25 min) in the anterior insular cortex (aIC), hippocampus (Hi), and anterior cingulate cortex (ACC; red; voxel-wise correlation with a threshold of $p < 0.05$).

(B) Correlation of the difference between delayed DA release after milkshake and tasteless solution intake (rDA; 35–40 min) in the putamen (Pu) with the wanting score (blue; voxel-wise correlation with a threshold of $p < 0.05$).

(C) Post hoc analysis revealing correlations between wanting scores and ΔrDA in aIC, Hi, ACC, and Pu.

(D) Correlation between DA release in wanting-associated areas at stimulus delivery with post-ingestive DA release in the putamen. The correlation was significant in both milkshake (triangle; $p = 0.008$, $r = -0.78$) and tasteless (circle; $p = 0.007$, $r = -0.78$) condition.

(E) Desire to eat is potentially linked to DA release in motivation-associated brain areas. Post-ingestive DA release in the putamen presumably inhibits desire to eat and hence DA release in wanting-related areas.

Therefore, although the amount of released DA is lower in extra-striatal regions, the major fraction is removed slowly and thereby contributes to variations in [^{11}C]raclopride binding. Simultaneous voltammetry recordings of evoked striatal and cortical DA release

in rats clearly show this effect: the amplitudes of release-induced minute-by-minute variations in extracellular DA concentrations are of the same order of magnitude in extra-striatal regions as in the striatum despite the difference in total amount of released

DA (Garris et al., 1993). This could explain the extrastriatal food-induced changes of rDA that we observed here.

In the present study, a novel method for the analysis of [¹¹C]raclopride was applied to assess stimulus-induced DA release in humans. The method introduces the parameter rDA, which is directly calculated from temporal variations in the [¹¹C]raclopride signal, as a measure for regional DA release. In the methodological paper we could demonstrate, with the help of voltammetry recordings in mice, that phasic DA release systematically induces minute-by-minute variations in extracellular DA concentrations, that these variations induce detectable variations in the [¹¹C]raclopride signal (as measured by rDA), and that the amplitude of these variations is proportional to the rates of phasic DA release (Lippert et al., 2018). In order to compare regional rDA values between subjects, it is imperative that the PET data were acquired under similar conditions (same scanner, specific activity of the tracer, etc.). Regarding the data shown in Figure 5, it appears that the determination of rDA is strikingly robust: each data point in Figure 5B indicates the difference between rDA during milkshake and tasteless solution condition in the same region for each individual subject (9 data points, one subject did not fill out the “wanting” data sheet). There was at minimum 1 week between the two PET sessions. In the four regions displayed, we found high correlations between the individual wanting scores and the individual difference of rDA. Each data point in Figure 5D displays rDA in the wanting-related regions (immediate) and in the putamen (post-ingestive) for each individual PET session (10 subjects * 2 sessions = 20 data points; the subject who did not fill out the “wanting” data sheet is also included here). These data indicate that post-ingestive rDA is only high if immediate rDA in wanting-related regions is low. Without providing solid proof, these results do indicate that rDA is reproducible. However, further studies are necessary to substantiate the utility of the method for the detection of DA release.

STAR★METHODS

Detailed methods are provided in the online version of this paper and include the following:

- KEY RESOURCES TABLE
- CONTACT FOR REAGENT AND RESOURCE SHARING
- EXPERIMENTAL MODEL AND SUBJECT DETAILS
- METHOD DETAILS
 - Experimental Design
 - Gustometer Setup
 - fMRI Data Acquisition
 - PET Data Collection
- QUANTIFICATION AND STATISTICAL ANALYSIS
 - fMRI Analysis
 - PET Analysis
 - Combined fMRI and PET Analysis
 - Reporting of Brain Areas
 - Other Statistical Analyses

SUPPLEMENTAL INFORMATION

Supplemental Information includes one figure and can be found with this article online at <https://doi.org/10.1016/j.cmet.2018.12.006>.

ACKNOWLEDGMENTS

The authors are especially grateful to Ivan de Araujo for his comments on an earlier version of the manuscript, to Henning Fenselau for providing his insight into gastric signaling, and to Henry Evrard for discussions on insular anatomy and its relevance in this work. Hendrik Nolte assisted with statistical analysis, Sonja Blum provided excellent technical assistance, and Bernd Neumaier together with the former Radiochemistry Lab at the Max Planck Institute for Neurological Research provided the PET tracer. H.B., M.T., and J.C.B. were supported by the German Research Foundation in the Transregional Collaborative Research Center 134. M.T. and J.C.B. are further supported by the German Centre for Diabetes Research.

AUTHOR CONTRIBUTIONS

S.E.T., J.C.B., D.M.S., and M.T. conceived the study; S.E.T. performed all experiments. S.E.T. and H.B. analyzed the data. A.G.D. provided support to establish the gustometer setup and A.L.C. as well as R.N.L. supported validation of the analysis technique. K.A., O.A.C., and R.H. contributed to participant recruitment as well as data acquisition. S.E.T., H.B., and M.T. wrote the manuscript. All authors agreed on the final version of the manuscript.

DECLARATION OF INTERESTS

The authors declare no competing interests.

Received: February 1, 2018

Revised: May 18, 2018

Accepted: December 4, 2018

Published: December 27, 2018

REFERENCES

- Adams, W.K., Sussman, J.L., Kaur, S., D'souza, A.M., Kieffer, T.J., and Winstanley, C.A. (2015). Long-term, calorie-restricted intake of a high-fat diet in rats reduces impulse control and ventral striatal D2 receptor signalling - two markers of addiction vulnerability. *Eur. J. Neurosci.* *42*, 3095–3104.
- Andersson, J.L.R., Skare, S., and Ashburner, J. (2003). How to correct susceptibility distortions in spin-echo echo-planar images: application to diffusion tensor imaging. *Neuroimage* *20*, 870–888.
- Andrews, Z.B., and Horvath, T.L. (2008). Tasteless food reward. *Neuron* *57*, 806–808.
- Assar, N., Mahmoudi, D., Farhoudian, A., Farhadi, M.H., Fatahi, Z., and Haghparast, A. (2016). D1- and D2-like dopamine receptors in the CA1 region of the hippocampus are involved in the acquisition and reinstatement of morphine-induced conditioned place preference. *Behav. Brain Res.* *312*, 394–404.
- Babbs, R.K., Sun, X., Felsted, J., Chouinard-Decorte, F., Veldhuizen, M.G., and Small, D.M. (2013). Decreased caudate response to milkshake is associated with higher body mass index and greater impulsivity. *Physiol. Behav.* *121*, 103–111.
- Baker, P.M., Jhou, T., Li, B., Matsumoto, M., Mizumori, S.J.Y., Stephenson-Jones, M., and Vicentic, A. (2016). The lateral habenula circuitry: reward processing and cognitive control. *J. Neurosci.* *36*, 11482–11488.
- Baldo, B.A., Sadeghian, K., Basso, A.M., and Kelley, A.E. (2002). Effects of selective dopamine D1 or D2 receptor blockade within nucleus accumbens subregions on ingestive behavior and associated motor activity. *Behav. Brain Res.* *137*, 165–177.
- Balleine, B.W., Delgado, M.R., and Hikosaka, O. (2007). The role of the dorsal striatum in reward and decision-making. *J. Neurosci.* *27*, 8161–8165.
- Bartoshuk, L.M., Duffy, V.B., Green, B.G., Hoffman, H.J., Ko, C.W., Lucchina, L.A., Marks, L.E., Snyder, D.J., and Weiffenbach, J.M. (2004). Valid cross-group comparisons with labeled scales: the gLMS versus magnitude matching. *Physiol. Behav.* *82*, 109–114.
- Beck, A.T., Steer, R.A., and Brown, G.K. (1996). Manual for the Beck Depression Inventory-II (Psychological Corporation).

- Berridge, K.C., and Robinson, T.E. (1998). What is the role of dopamine in reward: hedonic impact, reward learning, or incentive salience? *Brain Res. Brain Res. Rev.* **28**, 309–369.
- Beutler, L.R., Chen, Y., Ahn, J.S., Lin, Y.C., Essner, R.A., and Knight, Z.A. (2017). Dynamics of gut-brain communication underlying hunger. *Neuron* **96**, 461–475.e5.
- Brainard, D.H. (1997). The Psychophysics Toolbox. *Spat. Vis.* **10**, 433–436.
- Chen, X., Gabbito, M., Peng, Y., Ryba, N.J.P., and Zuker, C.S. (2011). A gustotopic map of taste qualities in the mammalian brain. *Science* **333**, 1262–1266.
- Chen, Y., Lin, Y.-C., Kuo, T.-W., and Knight, Z.A. (2015). Sensory detection of food rapidly modulates arcuate feeding circuits. *Cell* **160**, 829–841.
- Cizek, J., Herholz, K., Vollmar, S., Schrader, R., Klein, J., and Heiss, W.-D. (2004). Fast and robust registration of PET and MR images of human brain. *Neuroimage* **22**, 434–442.
- Cohen, M.X., Schoene-Bake, J.C., Elger, C.E., and Weber, B. (2009). Connectivity-based segregation of the human striatum predicts personality characteristics. *Nat. Neurosci.* **12**, 32–34.
- Cosgrove, K.P., Veldhuizen, M.G., Sandiego, C.M., Morris, E.D., and Small, D.M. (2015). Opposing relationships of BMI with BOLD and dopamine D2/3 receptor binding potential in the dorsal striatum. *Synapse* **69**, 195–202.
- de Araujo, I.E. (2016). Circuit organization of sugar reinforcement. *Physiol. Behav.* **164** (Pt B), 473–477.
- de Araujo, I.E., and Simon, S.A. (2009). The gustatory cortex and multisensory integration. *Int. J. Obes.* **33** (Suppl 2), S34–S43.
- de Araujo, I.E., Oliveira-Maia, A.J., Sotnikova, T.D., Gainetdinov, R.R., Caron, M.G., Nicolelis, M.A., and Simon, S.A. (2008). Food reward in the absence of taste receptor signaling. *Neuron* **57**, 930–941.
- de Araujo, I.E., Geha, P., and Small, D.M. (2012). Orosensory and homeostatic functions of the insular taste cortex. *Chemosens. Percept.* **5**, 64–79.
- de Araujo, I.E., Lin, T., Veldhuizen, M.G., and Small, D.M. (2013). Metabolic regulation of brain response to food cues. *Curr. Biol.* **23**, 878–883.
- Delgado, M.R., Stenger, V.A., and Fiez, J.A. (2004). Motivation-dependent responses in the human caudate nucleus. *Cereb. Cortex* **14**, 1022–1030.
- DiFeliceantonio, A.G., Coppin, G., Rigoux, L., Edwin Thanarajah, S., Dagher, A., Tittgemeyer, M., and Small, D.M. (2018). Supra-additive effects of combining fat and carbohydrate on food reward. *Cell Metab.* **28**, 33–44.e3.
- Evrard, H.C., Logothetis, N.K., and Craig, A.D. (2014). Modular architectonic organization of the insula in the macaque monkey. *J. Comp. Neurol.* **522**, 64–97.
- Ferreira, J.G., Tellez, L.A., Ren, X., Yeckel, C.W., and de Araujo, I.E. (2012). Regulation of fat intake in the absence of flavour signalling. *J. Physiol.* **590**, 953–972.
- Frank, S., Veit, R., Sauer, H., Enck, P., Friederich, H.C., Unholzer, T., Bauer, U.M., Linder, K., Heni, M., Fritsche, A., and Preissl, H. (2016). Dopamine depletion reduces food-related reward activity independent of BMI. *Neuropsychopharmacology* **41**, 1551–1559.
- Friston, K.J., Worsley, K.J., Frackowiak, R.S., Mazziotta, J.C., and Evans, A.C. (1994). Assessing the significance of focal activations using their spatial extent. *Hum. Brain Mapp.* **1**, 210–220.
- Garris, P.A., Collins, L.B., Jones, S.R., and Wightman, R.M. (1993). Evoked extracellular dopamine in vivo in the medial prefrontal cortex. *J. Neurochem.* **61**, 637–647.
- Green, B.G., Dalton, P., Cowart, B., Shaffer, G., Rankin, K., and Higgins, J. (1996). Evaluating the ‘Labeled Magnitude Scale’ for measuring sensations of taste and smell. *Chem. Senses* **21**, 323–334.
- Hajnal, A., Smith, G.P., and Norgren, R. (2004). Oral sucrose stimulation increases accumbens dopamine in the rat. *Am. J. Physiol. Regul. Integr. Comp. Physiol.* **286**, R31–R37.
- Han, W., Tellez, L.A., Niu, J., Medina, S., Ferreira, T.L., Zhang, X., Su, J., Tong, J., Schwartz, G.J., van den Pol, A., and de Araujo, I.E. (2016). Striatal dopamine links gastrointestinal rerouting to altered sweet appetite. *Cell Metab.* **23**, 103–112.
- Howe, M.W., and Dombeck, D.A. (2016). Rapid signalling in distinct dopaminergic axons during locomotion and reward. *Nature* **535**, 505–510.
- Hsiao, S., and Smith, G.P. (1995). Raclopride reduces sucrose preference in rats. *Pharmacol. Biochem. Behav.* **50**, 121–125.
- Jenkinson, M., Bannister, P., Brady, M., and Smith, S. (2002). Improved optimization for the robust and accurate linear registration and motion correction of brain images. *Neuroimage* **17**, 825–841.
- Johnson, P.M., and Kenny, P.J. (2010). Dopamine D2 receptors in addiction-like reward dysfunction and compulsive eating in obese rats. *Nat. Neurosci.* **13**, 635–641.
- Kaelberer, M.M., Buchanan, K.L., Klein, M.E., Barth, B.B., Montoya, M.M., Shen, X., and Bohórquez, D.V. (2018). A gut-brain neural circuit for nutrient sensory transduction. *Science* **361**, eaat5236.
- Kelley, A.E., Baldo, B.A., Pratt, W.E., and Will, M.J. (2005). Corticostriatal-hypothalamic circuitry and food motivation: integration of energy, action and reward. *Physiol. Behav.* **86**, 773–795.
- Kenny, P.J. (2011). Reward mechanisms in obesity: new insights and future directions. *Neuron* **69**, 664–679.
- Laruelle, M. (2000). Imaging synaptic neurotransmission with in vivo binding competition techniques: a critical review. *J. Cereb. Blood Flow Metab.* **20**, 423–451.
- Lim, J., Wood, A., and Green, B.G. (2009). Derivation and evaluation of a labeled hedonic scale. *Chem. Senses* **34**, 739–751.
- Lippert, R.N., Cremer, A.L., Thanarajah, S.E., Korn, C., Jahans-Price, T., Burgeno, L., Tittgemeyer, M., Brüning, J.C., Walton, M.E., and Backes, H. (2018). Time-dependent assessment of stimulus-evoked regional dopamine release. *Nat. Commun.* Published online December 27, 2018. <https://doi.org/10.1038/s41467-018-8143-4>.
- Liu, Y., Gao, J.H., Liu, H.L., and Fox, P.T. (2000). The temporal response of the brain after eating revealed by functional MRI. *Nature* **405**, 1058–1062.
- Livneh, Y., Ramesh, R.N., Burgess, C.R., Levandowski, K.M., Madara, J.C., Fenselau, H., Goldey, G.J., Diaz, V.E., Jikomes, N., Resch, J.M., et al. (2017). Homeostatic circuits selectively gate food cue responses in insular cortex. *Nature* **546**, 611–616.
- Lucas, F., and Sclafani, A. (1989). Flavor preferences conditioned by intragastric fat infusions in rats. *Physiol. Behav.* **46**, 403–412.
- Maffei, A., Haley, M., and Fontanini, A. (2012). Neural processing of gustatory information in insular circuits. *Curr. Opin. Neurobiol.* **22**, 709–716.
- Mai, J.K., Majtanik, M., and Paxinos, G. (2015). *Atlas of the Human Brain* (Academic Press).
- Mela, D.J. (2006). Eating for pleasure or just wanting to eat? Reconsidering sensory hedonic responses as a driver of obesity. *Appetite* **47**, 10–17.
- Murdaugh, D.L., Cox, J.E., Cook, E.W., 3rd, and Weller, R.E. (2012). fMRI reactivity to high-calorie food pictures predicts short- and long-term outcome in a weight-loss program. *Neuroimage* **59**, 2709–2721.
- Nichols, T., and Hayasaka, S. (2003). Controlling the familywise error rate in functional neuroimaging: a comparative review. *Stat. Methods Med. Res.* **12**, 419–446.
- O’Doherty, J.P., Deichmann, R., Critchley, H.D., and Dolan, R.J. (2002). Neural responses during anticipation of a primary taste reward. *Neuron* **33**, 815–826.
- Palminter, R.D. (2007). Is dopamine a physiologically relevant mediator of feeding behavior? *Trends Neurosci.* **30**, 375–381.
- Pignatelli, M., and Bonci, A. (2015). Role of dopamine neurons in reward and aversion: a synaptic plasticity perspective. *Neuron* **86**, 1145–1157.
- Polk, S.E., Schulte, E.M., Furman, C.R., and Gearhardt, A.N. (2017). Wanting and liking: Separable components in problematic eating behavior? *Appetite* **115**, 45–53.
- Robinson, M.J., Fischer, A.M., Ahuja, A., Lesser, E.N., and Maniates, H. (2016). Roles of “wanting” and “liking” in motivating behavior: gambling, food, and drug addictions. *Curr. Top. Behav. Neurosci.* **27**, 105–136.
- Rothmund, Y., Preuschhof, C., Böhner, G., Bauknecht, H.C., Klingebiel, R., Flor, H., and Klapp, B.F. (2007). Differential activation of the dorsal striatum

- by high-calorie visual food stimuli in obese individuals. *Neuroimage* **37**, 410–421.
- Schmahmann, J.D., and Pandya, D.N. (1997). Anatomic organization of the basilar pontine projections from prefrontal cortices in rhesus monkey. *J. Neurosci.* **17**, 438–458.
- Schneider, L.H. (1989). Orosensory self-stimulation by sucrose involves brain dopaminergic mechanisms. *Ann. N Y Acad. Sci.* **575**, 307–319, discussion 319–320.
- Sclafani, A., and Ackroff, K. (2012). Role of gut nutrient sensing in stimulating appetite and conditioning food preferences. *Am. J. Physiol. Regul. Integr. Comp. Physiol.* **302**, R1119–R1133.
- Sharpe, M.J., Marchant, N.J., Whitaker, L.R., Richie, C.T., Zhang, Y.J., Campbell, E.J., Koivula, P.P., Necarsulmer, J.C., Mejias-Aponte, C., Morales, M., et al. (2017). Lateral hypothalamic GABAergic neurons encode reward predictions that are relayed to the ventral tegmental area to regulate learning. *Curr. Biol.* **27**, 2089–2100.e5.
- Small, D.M., Gregory, M.D., Mak, Y.E., Gitelman, D., Mesulam, M.M., and Parrish, T. (2003a). Dissociation of neural representation of intensity and affective valuation in human gustation. *Neuron* **39**, 701–711.
- Small, D.M., Jones-Gotman, M., and Dagher, A. (2003b). Feeding-induced dopamine release in dorsal striatum correlates with meal pleasantness ratings in healthy human volunteers. *Neuroimage* **19**, 1709–1715.
- Small, D.M., Voss, J., Mak, Y.E., Simmons, K.B., Parrish, T., and Gitelman, D. (2004). Experience-dependent neural integration of taste and smell in the human brain. *J. Neurophysiol.* **92**, 1892–1903.
- Smith, S.M. (2002). Fast robust automated brain extraction. *Hum. Brain Mapp.* **17**, 143–155.
- Smith, G.P. (2004). Accumbens dopamine mediates the rewarding effect of orosensory stimulation by sucrose. *Appetite* **43**, 11–13.
- Sotak, B.N., Hnasko, T.S., Robinson, S., Kremer, E.J., and Palmiter, R.D. (2005). Dysregulation of dopamine signaling in the dorsal striatum inhibits feeding. *Brain Res.* **1061**, 88–96.
- Stice, E., Spoor, S., Bohon, C., and Small, D.M. (2008a). Relation between obesity and blunted striatal response to food is moderated by TaqIA A1 allele. *Science* **322**, 449–452.
- Stice, E., Spoor, S., Bohon, C., Veldhuizen, M.G., and Small, D.M. (2008b). Relation of reward from food intake and anticipated food intake to obesity: a functional magnetic resonance imaging study. *J. Abnorm. Psychol.* **117**, 924–935.
- Stoeckel, L.E., Weller, R.E., Cook, E.W., 3rd, Twieg, D.B., Knowlton, R.C., and Cox, J.E. (2008). Widespread reward-system activation in obese women in response to pictures of high-calorie foods. *Neuroimage* **41**, 636–647.
- Stuber, G.D., and Wise, R.A. (2016). Lateral hypothalamic circuits for feeding and reward. *Nat. Neurosci.* **19**, 198–205.
- Su, Z., Alhadeff, A.L., and Betley, J.N. (2017). Nutritive, post-ingestive signals are the primary regulators of AgRP neuron activity. *Cell Rep.* **21**, 2724–2736.
- Taber, M.T., and Fibiger, H.C. (1997). Activation of the mesocortical dopamine system by feeding: lack of a selective response to stress. *Neuroscience* **77**, 295–298.
- Tellez, L.A., Medina, S., Han, W., Ferreira, J.G., Licona-Limón, P., Ren, X., Lam, T.T., Schwartz, G.J., and de Araujo, I.E. (2013). A gut lipid messenger links excess dietary fat to dopamine deficiency. *Science* **341**, 800–802.
- Tellez, L.A., Han, W., Zhang, X., Ferreira, T.L., Perez, I.O., Shammah-Lagnado, S.J., van den Pol, A.N., and de Araujo, I.E. (2016). Separate circuitries encode the hedonic and nutritional values of sugar. *Nat. Neurosci.* **19**, 465–470.
- Tolhurst, G., Reimann, F., and Gribble, F.M. (2012). Intestinal sensing of nutrients. *Handb. Exp. Pharmacol.* (209), 309–335.
- van de Giessen, E., la Fleur, S.E., Eggels, L., de Bruin, K., van den Brink, W., and Booij, J. (2013). High fat/carbohydrate ratio but not total energy intake induces lower striatal dopamine D2/3 receptor availability in diet-induced obesity. *Int. J. Obes.* **37**, 754–757.
- Veldhuizen, M.G., Bender, G., Constable, R.T., and Small, D.M. (2007). Trying to detect taste in a tasteless solution: modulation of early gustatory cortex by attention to taste. *Chem. Senses* **32**, 569–581.
- Veldhuizen, M.G., Douglas, D., Aschenbrenner, K., Gitelman, D.R., and Small, D.M. (2011). The anterior insular cortex represents breaches of taste identity expectation. *J. Neurosci.* **31**, 14735–14744.
- Veldhuizen, M.G., Babbs, R.K., Patel, B., Fobbs, W., Kroemer, N.B., Garcia, E., Yeomans, M.R., and Small, D.M. (2017). Integration of sweet taste and metabolism determines carbohydrate reward. *Curr. Biol.* **27**, 2476–2485.e6.
- Volkow, N.D., Wang, G.J., Fowler, J.S., Logan, J., Jayne, M., Franceschi, D., Wong, C., Gatley, S.J., Gifford, A.N., Ding, Y.S., and Pappas, N. (2002). “Nonhedonic” food motivation in humans involves dopamine in the dorsal striatum and methylphenidate amplifies this effect. *Synapse* **44**, 175–180.
- Volkow, N.D., Wise, R.A., and Baler, R. (2017). The dopamine motive system: implications for drug and food addiction. *Nat. Rev. Neurosci.* **18**, 741–752.
- Wise, R.A., Spindler, J., deWit, H., and Gerberg, G.J. (1978). Neuroleptic-induced “anhedonia” in rats: pimozone blocks reward quality of food. *Science* **201**, 262–264.
- Woolrich, M.W., Jbabdi, S., Patenaude, B., Chappell, M., Makni, S., Behrens, T., Beckmann, C., Jenkinson, M., and Smith, S.M. (2009). Bayesian analysis of neuroimaging data in FSL. *Neuroimage* **45** (1, Suppl), S173–S186.
- Yeomans, M.R., Leitch, M., Gould, N.J., and Mobini, S. (2008). Differential hedonic, sensory and behavioral changes associated with flavor-nutrient and flavor-flavor learning. *Physiol. Behav.* **93**, 798–806.

STAR★METHODS

KEY RESOURCES TABLE

| REAGENT or RESOURCE | SOURCE | IDENTIFIER |
|---|---|---|
| Chemicals, Peptides, and Recombinant Proteins | | |
| [11C]Raclopride | Radio Chemistry Lab, Max Planck Institute for Neurological Research | N/A |
| Software and Algorithms | | |
| GraphPad Prism 7.0d | GraphPad Software | https://www.graphpad.com/scientific-software/prism/ |
| MATLAB 2014 | MathWorks | https://de.mathworks.com/products/matlab.html |
| FSL 5.0 | FMRIB Software Library | https://fsl.fmrib.ox.ac.uk/fsl/fslwiki |
| VINCI 4.9 | Max Planck Institute for Metabolism Research | http://vinci.sf.mpg.de/ |
| IDL 8.5.1 | Exelis Visual Information Solutions | https://www.harrisgeospatial.com/Software-Technology/IDL |
| Gcc 4.8.4 | Free Software Foundation | https://www.gnu.org/software/gcc/ |
| Numerical Recipes in C, 3 rd edition | Cambridge University Press | http://numerical.recipes/ |
| Veusz 1.18 | Jeremy Sanders and contributors | https://veusz.github.io/ |

CONTACT FOR REAGENT AND RESOURCE SHARING

Further information and requests for resources should be directed to and will be fulfilled by the Lead Contact, Heiko Backes (backes@sf.mpg.de).

EXPERIMENTAL MODEL AND SUBJECT DETAILS

Thirteen healthy volunteers of normal weight (BMI 25.57 ± 2.41 kg/m²) participated in the study. All participants were recruited from a preexisting database maintained at the Max Planck Institute for Metabolism Research. To follow regulations of the German radiation protection authorities (BfS) only male participants between 40 and 70 years (age: 56 ± 9.5 years) were included in the study; also, to fulfill legal requirements, these participants had not participated in any previous PET study. Furthermore, all participants were non-smokers without any history of neurological, psychiatric, metabolic or eating disorders. We excluded volunteers on special diets, showing gluten or lactose intolerance as well as those scoring on the Beck Depression Inventory (BDI II; [Beck et al., 1996](#)) higher than 12. All volunteers participated in the fMRI part of the study. Out of these, 10 (age: 57.1 ± 10.55 years, BMI 25.73 ± 2.67 kg/m²) additionally underwent two PET-measurements. In the course of the data analysis, one subject had to be excluded from the fMRI-analysis due to incomplete data-acquisition. All subjects gave written informed consent to participate in the experiment, which was approved by the local ethics committee of the Medical Faculty of the University of Cologne (Cologne, Germany; No. 16-320).

METHOD DETAILS

Experimental Design

The study was carried out in a controlled, randomized, crossover design ([Figure S1](#)). Each volunteer participated on three testing days starting around the same time on the testing day (either 8 a.m. or 9 a.m.). On each testing day, participants arrived fasted with the last meal before 10 p.m. of the previous day. At the beginning of each day an intravenous catheter was inserted in the right forearm vein. Adherence to overnight fast was controlled by sampling blood glucose and insulin level in baseline condition. To assess metabolic changes by milkshake consumption glucose sampling was repeated after each scan. In addition, we acquired triglycerides, cholesterol, cortisol as well as HbA1c levels on the first testing day in order to rule out metabolic diseases. After each blood draw, the participants were asked to rate their hunger, satiety, thirst, tiredness as well as their wish to eat on a 100 mm visual analog scale (0 = “not hungry/sated/tired at all” and 100 = “very hungry/sated/tired”).

On the first day, participants received training for using different rating scales with imagined stimuli. For the control condition, a solution was finally selected that the subjects indicated as tasteless during the test. Here, four different dilutions (100%, 75%,

50% and 25%) of the original solution (25 mM potassium chloride and 2.5 mM sodium bicarbonate) were presented pairwise. The solution selected in two successive comparisons was finally picked. Next, participants were presented four different milkshake flavors (vanilla, strawberry, banana, and chocolate). Here, the two milkshakes that were rated highest on liking and wanting were finally picked. Overall stimulus intensity as well as sweetness intensity were tested with the general labeled magnitude scale (gLMS; [Bar-toshuk et al., 2004](#); [Green et al., 1996](#)). Liking was rated on a vertical labeled hedonic scale ([Lim et al., 2009](#); upper anchor point = “most liked,” lower anchor point = “most disliked”) and wanting was rated on a 100 mm visual analog scale (upper anchor point = “I don’t want to drink the solution at all,” lower anchor point = “I want to drink the solution very much”). After each tasting, participants were instructed to rinse their mouth with a glass of water and wait one minute for the next trial. Only participants that at least moderately liked and wanted the milkshake were included in the study.

Subsequently, on the first testing day each chosen participant underwent fMRI acquisition. On the second and third testing day PET Scans were performed in a randomized order with participants either receiving the chosen milkshakes or tasteless solution during the scan.

Gustometer Setup

All participants were fitted with a custom designed Teflon mouth-piece for fluid delivery to the tongue tip that was attached to the head-coil (64-channel head coil; Siemens, Erlangen, Germany) or to PET gantry. The gustometer consisted of four programmable syringe pumps (LA-100, HLL Landgraf Laborsysteme, Langenhagen, Germany), each with a 50 mL syringe (Braun, Melsungen, Germany) that contained either one of the two selected milkshakes, tasteless solution or water. The syringes were connected to the mouth-piece via a silicon beverage tubing (Lindemann GmbH, Helmstedt) with an inside diameter of 2 mm. The syringe pumps were controlled by scripts written in MATLAB (The Mathworks, MATLAB version 2014b) using the psychophysics toolbox extension (version 3.0.11; [Brainard, 1997](#)). In two 8.37 min long sessions, participants received tasteless solution and both milkshakes in a randomized order. Each milkshake supply was followed by a water rinse. Moreover, 80% of the stimuli were predictable by an auditory cue and 20% of the supplies appeared unpredicted. The interval between cue and stimulus was programmed with a random exponential jitter of, on average, two seconds. Either a high tone (600 Hz) or a low tone (300 Hz) predicted the milkshake or the tasteless solution. The association between cue and stimulus remained constant across sessions; participants were informed about the tone-delivery association in the beginning of the scan through a standardized instruction.

fMRI Data Acquisition

The imaging was performed on a 3T MRI system (Siemens Magnetom Prisma, Erlangen, Germany) using a 64-channel head-coil. Two 8.37 min sessions were acquired of each subject. Gradient echo-planar images (EPI) with 34 slices (voxel size: 2.8x2.8x2.8 mm³, field of view: 220 mm, 2100 ms repetition time (TR), 30 ms echo time (TE), no distance factor) were acquired parallel to the commissural line (AC-PC) in a descending order from top to bottom. In addition, we acquired 2 short EPI-scans with 3 volumes each in opposing phase encoding directions (Anterior-Posterior, Posterior-Anterior) for later use in distortion correction. After each fMRI block a short anatomical scan was acquired (MPRAGE: 30 slices, voxel size: 2x2x2 mm³, field of view: 192x192 mm, TR = 250 ms, TE = 2.86 ms, no distance factor) for the purpose of registration to standard space (MNI). High-resolution T1-weighted images were acquired using a 12-channel array head coil with 128 sagittal slices and whole brain coverage on a different day (MDEFT3D: TR = 1930 ms, TI = 650 ms, TE = 5.8 ms, resolution 1x1x1.25 mm³, flip angle 18°).

PET Data Collection

PET imaging was acquired on a brain dedicated HRRT Siemens PET scanner. Each scan lasted 60 min. Participants were instructed not to sleep and to lie still. We injected 220-370 MBq [¹¹C]raclopride using a programmable syringe pump (Perfusor compact, Braun, Melsungen): 70% was applied in a bolus within the first minute, 30% was constantly infused during the remaining 59 min. To ensure steady state and acquire dynamic PET-data, the gustometer task started 20 min after the onset of data collection and lasted 10 min. The PET scan was continued for 30 min after task completion. Since we wanted to analyze time-dependent DA release following food intake we performed two different PET imaging sessions with either milkshake or tasteless solution in a randomized order. Each milkshake or tasteless supply was followed by a rinse of water.

QUANTIFICATION AND STATISTICAL ANALYSIS

fMRI Analysis

The individual datasets were preprocessed before running statistical analyses using tools from the FMRIB software Library (FSL version 5.0.8, <https://fsl.fmrib.ox.ac.uk/fsl/fslwiki>): time series were first re-aligned to correct for small head movements using MCFLIRT ([Jenkinson et al., 2002](#)). Non-brain tissues were removed using an automated brain extraction tool (BET; [Smith, 2002](#)). For distortion correction, we collected pairs of images with distortions going in opposite phase encoding directions. From these pairs, the susceptibility-induced off-resonance field was estimated using the topup tool as implemented in FSL ([Andersson et al., 2003](#)). The FEAT package within FSL was used for single- and group level analysis. Slice time correction, Gaussian smoothing with a 6 mm FWHM kernel and high pass temporal filtering (FWHM = 120 s) was performed for each session. The EPI-images were first

registered to the individual anatomical T1-weighted scan and subsequently to the MNI-152 standard brain. Additionally, we extracted time series of white matter in both hemispheres, and the ventricle to account for possible confounds. Since stimuli were presented repeatedly in blocks, a block-related model was used in the GLM analysis. Predicted and unpredicted trials were collapsed. A boxcar convolved with a double gamma hemodynamic response function (HRF) was used to model the data. To detect areas that responded to milkshake we obtained the contrast “milkshake-tasteless” for each session. In the second level analysis, both sessions of each subject were included and analyzed with a fixed effect model. On group level, we performed a mixed effect model analysis with Bayesian estimation techniques using FLAME (FMRIB’s Local Analysis of Mixed Effects; Woolrich et al., 2009) stage 1 and 2 to test for the average effect across the group. Age and BMI were included as covariates after demeaning. Gaussian random field theory was applied for cluster-based correction for multiple comparisons resulting in thresholded z-score maps. Note that we only report data that survived cluster level correction (z-threshold = 2.3, cluster significance p-threshold = 0.05, corrected) in whole brain analysis.

PET Analysis

After correcting for attenuation and scatter, PET images were reconstructed in 12 time intervals of 5 min duration using three-dimensional ordinary Poisson ordered subset expectation maximization (OP-3D-OSEM) including the modeling of the system’s point spread function (PSF). Individual PET images were smoothed by application of a 10 mm Gaussian filter and co-registered with respective T1-weighted MR image using the imaging software VINCI (Cizek et al., 2004). The individual MR images were then non-linearly transformed into the stereotaxic Montreal Neurological Institute (MNI) space and the transformation matrix was applied to the corresponding multiframe PET images (VINCI). [11C]raclopride PET data were analyzed following a newly developed approach. Details of the method are published in a separate methodological paper (Lippert et al., 2019). In brief, [11C]raclopride predominantly binds to extrasynaptic extracellular D2 receptors and thereby competes with endogenous extracellular DA levels. We have shown that activation of DA neurons not only induces synaptic DA transmission and corresponding extracellular DA transients (timescale ~1 s), but also induces low frequency variations of DA levels in extracellular space. We further showed that the amplitude of low and high frequency variations of DA are linearly correlated. Low frequency variations of extracellular DA cause variations of the amount of D2 receptor-bound DA levels, which interact with the binding of [11C]raclopride. Therefore low frequency (~minutes) variations of [11C]raclopride in tissue are related to low frequency variations of DA (and also to the correlated high frequency variations) and can be used as a quantitative measure for dopaminergic activity. The parameter rDA, which has been shown to be a measure for transient dopamine release rates, is calculated from the [11C]raclopride PET data as

$$rDA_{ijk}(t_n) = \frac{1}{R_{0,ijk}} \sqrt{\frac{1}{125} \sum_{u=i-2}^{i+2} \sum_{v=j-2}^{j+2} \sum_{w=k-2}^{k+2} (R_{uvw}(t_n) - R_{uvw}(t_{n-1}))^2}$$

$$R_{0,ijk} = \frac{1}{8} \frac{1}{125} \sum_{n=5}^{12} \sum_{u=i-2}^{i+2} \sum_{v=j-2}^{j+2} \sum_{w=k-2}^{k+2} R_{uvw}(t_n)$$

with $R_{ijk}(t_n)$ the [11C]raclopride PET signal in voxel i,j,k at time t_n (Lippert et al., 2019). Calculation of dopaminergic activity (rDA) from the [11C]raclopride data requires quasi-steady state conditions. To fulfill this prerequisite, we inject [11C]raclopride by a bolus plus infusion method. A quasi-steady state is then reached after ~15 min. After this time, the new method provides spatio-temporal maps of rDA at a temporal resolution of 5 min and a spatial resolution of ~1 mL. Note, that PET tracer delivery by a bolus plus constant infusion method has the merit of making the PET signal insensitive to variations in blood flow (Laruelle, 2000). We can therefore rule out that the observed alterations in the [11C]raclopride PET signal could have been caused by changes in blood flow.

In order to identify regions with differences in rDA depending on food intake (tasteless solution or milkshake) we performed voxel-wise paired t tests and found clusters of contiguous voxels with $p(\text{uncorrected}) < 0.05$. Random field theory-based correction for multiple comparisons was performed by calculating the family-wise error-corrected p value for the most significant voxel for each cluster with the whole brain as search volume (Nichols and Hayasaka, 2003). Additionally we performed family-wise error correction taking into account the cluster extent (Friston et al., 1994).

To identify regions where rDA depends on the subjective desire to eat we performed a voxel-wise correlation analysis (Pearson) between the change in rDA after milkshake versus tasteless solution intake (ΔrDA) and the wanting score. From this, clusters of contiguous voxels with $p < 0.05$ were identified. The Pearson correlation coefficients and p values were then calculated for each cluster.

Combined fMRI and PET Analysis

To identify brain areas that showed both a BOLD signal and DA release we extracted the z-statistics of group level fMRI analysis for the contrast “milkshake-tasteless” and constructed an overlap map with the group statistics of DA release. For this comparison, only the early time interval (0-5 min) in the PET data was selected that corresponds to the immediate response to milkshake consumption acquired in fMRI.

Reporting of Brain Areas

Coordinates of all brain areas that have been annotated in figures and reported in tables as results of our analysis have been carefully compared to the atlas provided by [Mai et al. \(2015\)](#).

Other Statistical Analyses

The analyses of biochemical data and ratings were performed using GraphPad Prism (vers. 6.0h, GraphPad Software, San Diego California USA, <https://www.graphpad.com/>).